LITHIUM NIOBATE ON SILICON LAMB MODE ACOUSTOELECTRIC WAVEGUIDE WITH 5.5 DB SUSTAINED TERMINAL GAIN

Hakhamanesh Mansoorzare and Reza Abdolvand
University of Central Florida, Orlando, Florida, USA

ABSTRACT

In this work, sustained terminal gain is reported for the first time in micromachined lithium niobate (LN) on silicon (Si) Lamb mode waveguides through acoustoelectric amplification. In such acoustically thin waveguides, the large coupling between the Lamb waves and the drifting electrons in Si gives rise to a very efficient transfer of momentum from electrons to elastic phonons, rendering the waveguide a traveling wave amplifier. In a geometrically optimized waveguide, up to 5.5 dB terminal gain is achieved by dissipating less than 6.5 milliwatts of DC bias power. This is measured for input RF signals up to -20 dBm and gain compression is observed for larger inputs with its characteristic impacted by the DC bias level and the device geometry. Further design improvements are expected to increase the terminal gain, hence, justifying the implementation of micro-acoustic RF amplifiers.

KEYWORDS

Acoustoelectric effect; heterostructure; Lamb wave; lithium niobate; piezoelectric; terminal gain; traveling wave amplifier.

INTRODUCTION

It has been known for decades that transistor-less signal amplification within the acoustic domain can be realized through the acoustoelectric (AE) effect [1]. Once charge carriers at the vicinity of piezoelectrically transduced acoustic waves move faster than the acoustic waves, they could transfer their momentum and amplify the acoustic waves. This phenomenon could be considered an acoustic equivalent to electromagnetic (EM) traveling wave tube amplifiers (TWTA). In a TWTA, a beam of drifting electrons amplifies a slow RF signal that is guided in its proximity within a helix wire or EM resonant cavity [2]. Similarly, in a piezoelectric semiconductor or layered piezoelectric/semiconductor system, drifting electrons could amplify an RF signal that is piezoelectrically transduced into a traveling wave, once they start leading such wave. While originally demonstrated in piezoelectric semiconductors, the acoustic wave amplification required prohibitively large voltages because of the low charge carrier mobility in such materials. Adopting a separate piezoelectric/semiconductor structure allowed for independent optimization of the piezoelectric and semiconductor properties, thus, improving device performance. To efficiently couple the semiconductor with the acoustic waves, surface acoustic waves (SAW) were utilized; for the first time, SAW was excited using a patterned electrode structure that conforms to the SAW wavelength. This led to numerous demonstrations of SAW AE devices comprising piezoelectric substrates and a thin layer of semiconductor that is either deposited or bonded on top of it or held at an infinitesimally small distance from its surface. The former approach allows for a stronger coupling between the charge carriers in semiconductor and SAW, since the evanescent electric field of SAW is confined in the semiconductor rather than being in the air gap. Additionally, the direct film deposition or bonding makes fabrication less complex since the need for nanometer-scale spacers is avoided. However, the deposited or bonded film must be extremely thin for minimizing the mechanical perturbation of SAW. Even with the deposition and bonding processes that are available today, attaining a high carrier mobility in an ultra-thin film remains challenging. Furthermore, the operation frequency of SAW is practically up to ~3 GHz, before surface losses and small features in lithography become limiting. Owing to the recent progress in thin-film deposition and bonding, as well as high piezoelectric couplings provided by lithium niobate (LN), significant improvements in performance of SAW AE devices have been reported [3, 4, 5]. Suspended thin-film LN can support Lamb waves with higher phase velocities compared to SAW, therefore, allowing for higher frequency operation [6]. More importantly, thanks to the large electromechanical coupling of some of these modes and low energy leakage in the suspended structure, this platform has offered superior performance in terms of bandwidth and loss [7]. Therefore, thin-film piezoelectric-on-semiconductor platform has been investigated for realizing AE devices that could enable higher frequency, wider bandwidth, and lower loss compared to traditional SAW counterparts [8, 9, 10]. In this regard, LN on silicon (Si) platform has shown promising performance by leveraging the high coupling of fundamental symmetric (S0) mode; this includes non-reciprocal transmission with more than 30 dB contrast [11] and with more than 33% 6-dB fractional bandwidth [12]. In this work, we aim to explore the potential of this platform in ultimately functioning as a transistor-less amplifier. Through optimization of the device geometry, we present for the first time, up to 5.5 dB sustained terminal gain with no pulsed-operation requirement. This is realized by consuming only a few milliwatts of DC power pumped into the Si layer and for up to -20 dBm continuous wave 613 MHz signal.

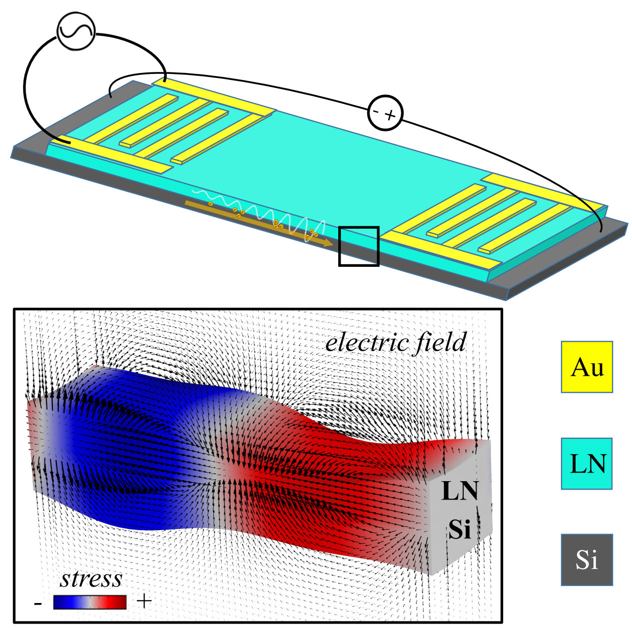

Figure 1: Schematic of suspended LN-on-Si waveguide for AE amplification; the RF signal is amplified by the DC voltage applied to Si. The S0 mode stress and electric field within a wavelength is shown in the inset.

METHODS

The fundamental parameter which determines the AE intensity is the coupling between the acoustic waves, S0 mode herein, and the electrons. This is a function of the piezoelectric coupling and the spatial arrangement of the acoustic waves and electrons. Therefore, to attain sufficient signal amplification that not only compensates the losses in the passive LN-on-Si waveguide, but also yields a terminal gain with low DC power budget, the AE coupling must be maximized. This translates into choosing a LN cut/orientation that supports the S0 mode with highest electromechanical coupling and a Si thickness that on one hand does not significantly reduce the electromechanical coupling of the heterostructure and on the other hand provides a sufficient spatial overlap between the drifting electrons and evanescent electric field. Since such evanescent field effectively extends by $1/k_0$ (with k_0 being the acoustic wavenumber), its penetration in Si would be smaller than ~1.6 µm at the acoustic wavelength of this study which is 10 µm. Additionally, to effectively excite the S0 mode, the heterostructure must be acoustically thin. Taking these into consideration, a stack of 1 µm LN on 1 µm Si is chosen for this study. The device schematic as well as the S0 mode stress profile and electric field within a wavelength, simulated by COMSOL, is shown in Fig. 1.

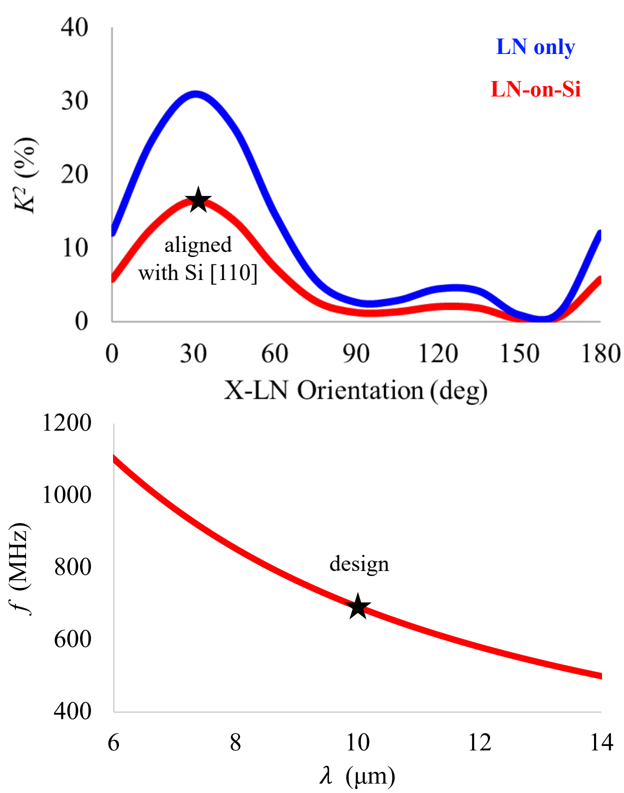

Figure 2: The electromechanical coupling dispersion for 1 µm X-cut LN with/without 1 µm Si for different LN orientations aligned with [110] Si (top). Frequency dispersion for Y30° orientation simulated by COMSOL (bottom).

Among the different cuts of LN, the X-cut LN offers the highest coupling for S0 mode once the acoustic wave propagates in ~30º off Y-axis direction [6]. Fig. 2 shows the electromechanical coupling dispersion of the stack vs. the LN orientation. This is calculated from the S0 phase velocity change because of short/open electrical boundary conditions on LN surface in COMSOL. Note that the addition of Si roughly reduces the electromechanical coupling from 31% to 16% at the optimal orientation. The frequency dispersion of said orientation is also plotted in Fig. 2; from this basic model, the wavelength targeted in this study should result in a passband frequency around ~670 MHz. The estimated electromechanical coupling along with the electrical properties of the stack is used to analytically predict the AE loss/gain from the model presented in [13]. This is shown in Fig. 3; without any external drift field, an AE loss of ~40 dB/mm is expected. Increasing the drift field so that the electron drift velocity reaches the Lamb wave phase velocity, at ~48 V/mm, would eliminate the AE loss, leaving the other less significant sources of loss to become dominant. This comprises the propagation loss in LN, LN-Si interface loss, and transducer electrode loss. Consequently, terminal gain would be possible at a drift field that yields an AE gain which covers all such losses. Limiting the available drift field to ~150 V/mm, up to ~70 dB/mm AE gain is possible. On the other hand, the rest of the loss sources are estimated to be less than 20 dB, which implies a waveguide having a length in the order of 500 µm could provide a 15 dB terminal gain. This, however, ignores the large signal effects and thermal issues that might arise at such high electric field levels.

The drift field is created by applying a voltage across the waveguide using DC contacts to Si outside of the acoustic propagation region. This is an advantage of the Lamb wave platform compared to SAW; in the latter, the semiconductor film and its DC access cause SAW perturbation as they lie within its propagation path. The devices are fabricated in a five-mask process starting with the bonded LN-on-SOI wafer which is provided by NGK Insulators LTD. Interdigital transducers (IDT) made of chromium/gold (25/75 nm) are deposited and patterned via e-beam evaporation and lift-off. Electrical contact points to Si for applying DC voltage are created outside of the waveguide by etching the LN layer. These openings and the RF probe pads are overlaid with another chromium/gold stack. The device boundaries are etched in ICP/RIE using argon (for LN) and DRIE (for Si) with a silicon dioxide mask. The devices are finally released from the backside by etching the Si handle layer and the buried oxide layer in DRIE and buffered oxide etchant, respectively.

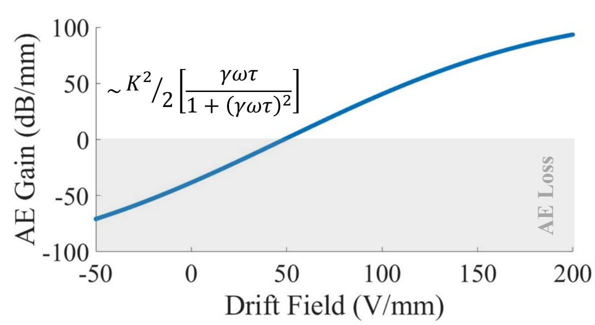

Figure 3: The analytical AE gain as a function of the applied drift field from the simple RC model presented in [13].

RESULTS

The fabricated waveguides have a width of either 150 or 300 µm while their length, being defined as the distance between the two ports IDT, ranges from 400 to 800 µm in 100 µm increments. The measurements are performed using a network analyzer in atmospheric pressure and at room temperature for input signals with -20 dBm power. The transmission response of two 500 µm long waveguides having different widths is shown in Fig. 4, once biased at 0 V (black) and 125 V (red). The 150 μm wide device shows a maximum insertion loss (IL) improvement of 17.3 dB (going from 31 to 13.7) and the IL of the 300 μm wide waveguide after 39.6 dB AE gain improves from 38.7 to -0.9 dB, thus yielding a 0.9 dB terminal gain. Note that the transmission responses are reported for impedance matched terminations since the IDT impedance is not specifically designed for 50 Ohms. This can be seen from the reflection at the input port of the waveguides once they are terminated with 50 Ohms (Fig 4).

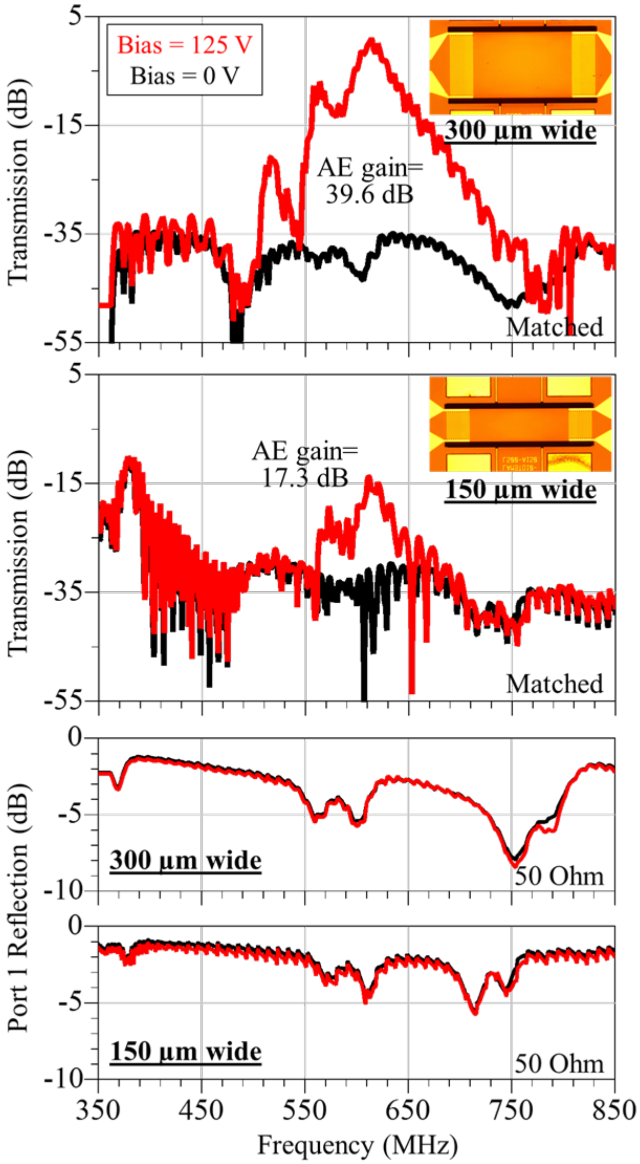

Figure 4: Measured transmission and reflection of waveguides having different widths and same lengths (500 μm) with 125 V bias (red) and no bias (black). The transmissions are reported with matched terminations.

A larger terminal gain is realized in a longer waveguide. This is shown in Fig. 5 for a 600 μm long, 300 μm wide device where the measured transmission responses at few bias points are plotted. By increasing the bias from the lowest to the highest voltage, the IL is improved from 36.8 dB to -5.5 dB, yielding 42.3 dB AE gain and 5.5 dB terminal gain. Keeping the voltage level limited to 125 V, devices with shorter or longer lengths demonstrate lower AE gain, making 600 μm close to the optimal device length. The 5.5 dB measured terminal gain is sustained by a constant DC bias of 125 V and 50 μA – i.e., dissipated power of ~6.25 mW – and is measured for a continuous wave at 613 MHz. As shown in Fig. 5, at this bias, the IL<0 passband has a span of ~30 MHz.

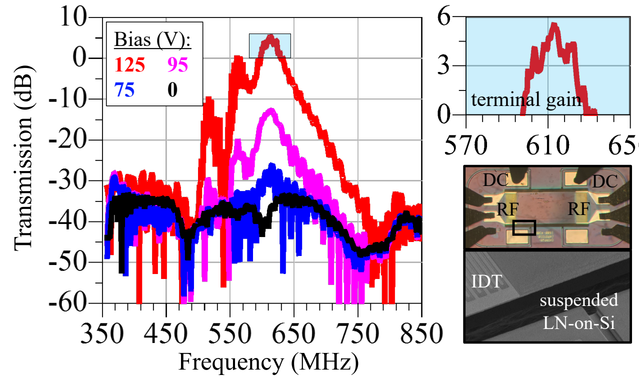

Figure 5: Measured transmission of the waveguide with optimal length (600 μm) showing an AE gain of 42.3 dB which results in 5.5 dB terminal gain with a continuous DC bias of 125V × 50μA.

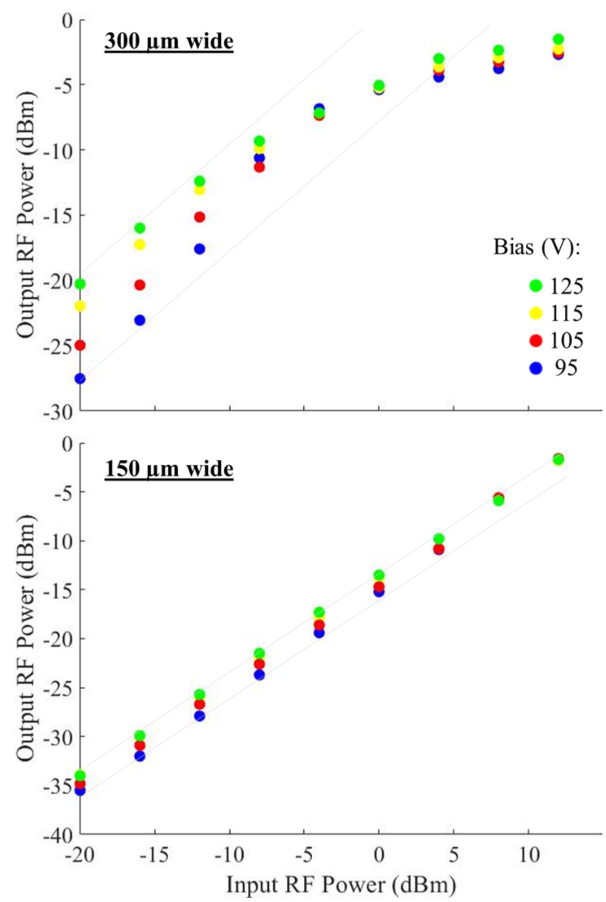

Figure 6: AE gain compression characteristic of waveguides having different widths and same lengths (500 μm). The wider device demonstrates larger gains but more non-linearity.

The measurements so far have been reported for RF input signals at -20 dBm and for larger input signals, the AE gain drops. The gain compression, furthermore, is observed to be affected by the device geometry and the bias level. This is shown in Fig. 6 for the two 500 µm long waveguides of Fig. 4. The input RF power is increased from -20 dBm to +12 dBm while the output power is recorded. The measurements are repeated for several bias levels. Although larger AE gains are measured in the wider device, the AE gain compression starts at lower RF input powers; the narrower device, on the other hand, shows a much more linear gain behavior in the measurement range and across the different bias levels.

CONCLUSIONS

The terminal gain, measured in this work, for continuous waves in micro-acoustic waveguides that are biased with a constant DC voltage, suggests the possibility of implementing more efficient amplifiers with better power handing using Lamb waves in lithium niobate on silicon thin films. Performance improvements are expected by further reducing the silicon thickness and optimizing the electrode design and the fabrication process. Having amplification capabilities in the micro-acoustic domain, where the majority of today's RF signal processing takes place, could lead to single-chip realization of more complex signal processing architectures, and eliminate the need for transistors in some applications.

ACKNOWLEDGEMENTS

This work was supported by the National Science Foundation (NSF) under award 2122670.

REFERENCES

[1] Y. V. Gulyaev and F. S. Hickernell, "Acoustoelectronics: history, present state, and new ideas for a new era," IEEE Ultrasonics Symposium, 2004.

[2] R. Kompfner, "Travelling-wave tubes." Reports on Progress in Physics 15.1, 1952.

[3] S. Ghosh and M. Ricci, "A 3-Port Circulator Based on Non-Reciprocal Acoustoelectric Delay Lines," 2020 Joint Conference of the IEEE International Frequency Control Symposium and International Symposium on Applications of Ferroelectrics (IFCS-ISAF), 2020.

[4] D. C. Malocha, C. Carmichael and A. Weeks, "Acoustoelectric Amplifier With 1.2-dB Insertion Gain Monolithic Graphene Construction and Continuous Wave Operation," in IEEE Trans. on Ultrasonics, Ferroelectrics, and Frequency Control, vol. 67, no. 9, pp. 1960-1963, Sept. 2020.

[5] L. Hackett, et al. "Towards single-chip radiofrequency signal processing via acoustoelectric electron–phonon interactions," Nature communications, vol. 12, no. 1, May 2021.

[6] I. E. Kuznetsova, B. D. Zaitsev, S. G. Joshi and I. A. Borodina, "Investigation of acoustic waves in thin plates of lithium niobate and lithium tantalate", IEEE Trans. Ultrason. Ferroelectr. Freq. Control, vol. 48, no. 1, pp. 322-328, Jan. 2001.

[7] R. Lu, and S. Gong, "RF acoustic microsystems based on suspended lithium niobate thin films: Advances and outlook." Journal of Micromechanics and Microengineering, vol. 31, no. 11, Sept. 2021.

[8] H. Mansoorzare and R. Abdolvand, "Acoustoelectric Amplification in Lateral-Extensional Composite Piezo-Silicon Resonant Cavities," 2019 Joint Conference of the IEEE International Frequency Control Symposium and European Frequency and Time Forum (EFTF/IFC), 2019.

[9] F. Hakim, M. Ramezani, S. Rassay and R. Tabrizian, "Non-Reciprocal Acoustoelectric Amplification in Germanium-Based Lamb Wave Delay Lines," 2019 IEEE International Electron Devices Meeting (IEDM), 2019.

[10] H. Mansoorzare and R. Abdolvand, "Acoustoelectric Non-Reciprocity in Lithium Niobate-on-Silicon Delay Lines," IEEE Electron Device Letters, vol. 41, no. 9, pp. 1444-1447, Jul. 2020.

[11] H. Mansoorzare and R. Abdolvand, "A Thin-Film Piezo-Silicon Acoustoelectric Isolator with More than 30 dB Non-Reciprocal Transmission," IEEE 34th International Conference on Micro Electro Mechanical Systems (MEMS), 2021.

[12] H. Mansoorzare and R. Abdolvand, "Ultra-Wideband Non-Reciprocal Micro-Acoustic Delay Lines with Slanted-Finger Interdigital Transducers," 2022 IEEE 35th International Conference on Micro Electro Mechanical Systems Conference (MEMS), 2022.

[13] R. Adler, "Simple theory of acoustic amplification." IEEE Transactions on Sonics and Ultrasonics 18.3, 1971.

CONTACT

*H. Mansoorzare, tel: +1-352-346-4400; hakha@knights.ucf.edu